

Ablation of Hepatocyte *Smad1*, *Smad5*, and *Smad8* Causes Severe Tissue Iron Loading and Liver Fibrosis in Mice

Chia-Yu Wang ,¹ Xia Xiao,¹ Abraham Bayer,¹ Yang Xu,¹ Som Dev,¹ Susanna Canali,¹ Anil V. Nair,¹ Ricard Masia,² and Jodie L. Babitt¹

A failure of iron to appropriately regulate liver hepcidin production is central to the pathogenesis of hereditary hemochromatosis. SMAD1/5 transcription factors, activated by bone morphogenetic protein (BMP) signaling, are major regulators of hepcidin production in response to iron; however, the role of SMAD8 and the contribution of SMADs to hepcidin production by other systemic cues remain uncertain. Here, we generated hepatocyte *Smad8* single (*Smad8^{f/f};Alb-Cre⁺*), *Smad1/5/8* triple (*Smad158;Alb-Cre⁺*), and littermate *Smad1/5* double (*Smad15;Alb-Cre⁺*) knockout mice to investigate the role of SMAD8 in hepcidin and iron homeostasis regulation and liver injury. We found that *Smad8;Alb-Cre⁺* mice exhibited no iron phenotype, whereas *Smad158;Alb-Cre⁺* mice had greater iron overload than *Smad15;Alb-Cre⁺* mice. In contrast to the sexual dimorphism reported for wild-type mice and other hemochromatosis models, hepcidin deficiency and extrahepatic iron loading were similarly severe in *Smad15;Alb-Cre⁺* and *Smad158;Alb-Cre⁺* female compared with male mice. Moreover, epidermal growth factor (EGF) failed to suppress hepcidin in *Smad15;Alb-Cre⁺* hepatocytes. Conversely, hepcidin was still increased by lipopolysaccharide in *Smad158;Alb-Cre⁺* mice, although lower basal hepcidin resulted in lower maximal hepcidin. Finally, unlike most mouse hemochromatosis models, *Smad158;Alb-Cre⁺* developed liver injury and fibrosis at 8 weeks. Liver injury and fibrosis were prevented in *Smad158;Alb-Cre⁺* mice by a low-iron diet and were minimal in iron-loaded *Cre⁻* mice. **Conclusion:** Hepatocyte *Smad1/5/8* knockout mice are a model of hemochromatosis that encompasses liver injury and fibrosis seen in human disease. These mice reveal the redundant but critical role of SMAD8 in hepcidin and iron homeostasis regulation, establish a requirement for SMAD1/5/8 in hepcidin regulation by testosterone and EGF but not inflammation, and suggest a pathogenic role for both iron loading and SMAD1/5/8 deficiency in liver injury and fibrosis. (HEPATOLOGY 2019;70:1986-2002).

Iron is tightly regulated for its functional necessity to most living organisms but toxicity when in excess. The iron hormone hepcidin controls systemic iron homeostasis by triggering degradation

of the iron exporter ferroportin, thereby limiting iron entry into the circulation.⁽¹⁾ The importance of hepcidin was recognized when mutations were linked to juvenile hemochromatosis, characterized

Abbreviations: Alb, albumin; ALK3, activin receptor-like kinase 3 (also known as *Bmpr1a*, bone morphogenetic receptor type Ia); ALT, alanine aminotransferase; ANOVA, analysis of variance; BMP, bone morphogenetic protein; Col1a1, collagen type I alpha 1; Cre, cyclization recombinase; EGF, epidermal growth factor; EGFR, EGF receptor; FBS, fetal bovine serum; Hamp, hepcidin antimicrobial peptide; HFE, homeostatic iron regulator; HJV, hemojuvelin; IL-6, interleukin-6; LPS, lipopolysaccharide; PBS, phosphate-buffered saline; Rpl19, ribosomal protein L19; R-SMAD, receptor-activated SMAD transcription factor; *Smad8^{f/f};Alb-Cre⁺*, hepatocyte *Smad8* single knockout mice; *Smad158;Alb-Cre⁺*, hepatocyte *Smad1*, *Smad5*, and *Smad8* triple knockout mice; *Smad15;Alb-Cre⁺*, hepatocyte *Smad1* and *Smad5* double knockout mice; STAT, signal transducer and activator of transcription; TFR2, transferrin receptor 2; *Tfsat*, transferrin saturation.

Received October 4, 2018; accepted May 17, 2019.

Additional Supporting Information may be found at onlinelibrary.wiley.com/doi/10.1002/hep.30780/supinfo.

Supported by the National Institutes of Health (RO1-DK087727, to J.L.B.) and in part by a Cooley's Anemia Foundation Research Fellowship (to C.-Y.W.).

© 2019 by the American Association for the Study of Liver Diseases.

View this article online at wileyonlinelibrary.com.

DOI 10.1002/hep.30780

Potential conflict of interest: Dr. Babitt consults for Disc Medicine and Keryx. She owns stock and has intellectual property rights with Ferrumax.

by early-onset tissue iron loading that leads to organ dysfunction including cirrhosis, hypogonadism, cardiomyopathy, and diabetes mellitus.⁽²⁾ Subsequently, the inability of iron to appropriately induce hepcidin was recognized as the common pathogenic mechanism for other genetic causes of hemochromatosis, including homeostatic iron regulator (*HFE*), transferrin receptor 2 (*TFR2*), and hemojuvelin (*HJV*) mutations.⁽³⁾

Bone morphogenetic protein (BMP)–SMAD signaling is a central pathway for hepcidin regulation by iron.⁽⁴⁾ Tissue iron stores induce BMP6 and BMP2 ligand expression in liver endothelial cells.⁽⁵⁻⁷⁾ Secreted BMPs bind type I and type II BMP receptors and the coreceptor *HJV* on hepatocytes to phosphorylate receptor-activated SMAD transcription factors (R-SMADs), which complex with the common mediator SMAD4, bind the hepcidin promoter, and induce transcription.⁽⁴⁾ *HFE* and *TFR2*, which are implicated in sensing serum iron levels,⁽⁴⁾ are also thought to regulate hepcidin by interacting with the SMAD signaling pathway.⁽⁸⁻¹¹⁾

In addition to iron, numerous other systemic cues are integrated by the liver to regulate hepcidin production.⁽¹²⁾ Inflammation induces hepcidin to limit iron availability to infectious microorganisms.⁽¹²⁾ Erythropoietic demand suppresses hepcidin to increase iron availability for erythropoiesis.⁽¹²⁾ Both testosterone and estrogen suppress hepcidin expression but through different mechanisms, which may help explain sex differences in iron loading and liver disease progression in hemochromatosis patients.⁽¹³⁻¹⁶⁾ Several growth factors, including epidermal growth factor (EGF) and hepatocyte growth factor (HGF), also suppress liver hepcidin production.⁽¹⁷⁾ Interestingly, many of these systemic signals are reported to intersect with the BMP-SMAD

pathway to regulate hepcidin, although the molecular mechanisms are not fully understood.⁽⁴⁾

Inflammation increases hepcidin production primarily by inducing interleukin-6 (IL-6), which activates signal transducer and activator of transcription 3 (STAT3) phosphorylation to stimulate hepcidin transcription.⁽¹²⁾ BMP R-SMAD phosphorylation is also activated by inflammation,^(18,19) and inhibiting BMP-SMAD signaling lowers hepcidin in the context of inflammation,⁽²⁰⁻²³⁾ suggesting crosstalk between the IL-6-STAT3 and BMP-SMAD pathways. One mechanism proposed for this crosstalk is inflammatory-mediated induction of the BMP/transforming growth factor beta (TGF- β) superfamily ligand activin B, which can use BMP type I receptors to phosphorylate BMP R-SMADs and induce hepcidin in hepatocytes.^(18,19) However, inflammation still induces hepcidin in activin B knockout mice,⁽²⁴⁾ raising questions about the contribution of this pathway *in vivo*. STAT3 and SMADs were also proposed to interact at the hepcidin promoter.⁽²⁵⁾ However, the functional contribution of BMP R-SMADs to hepcidin induction by inflammation *in vivo* has not been definitively demonstrated.

Compared with female mice, male mice exhibit lower basal hepcidin and more severe hepcidin deficiency and consequent extrahepatic iron loading in many hemochromatosis models.^(5,6,15,26) Testosterone was demonstrated to account for these observed sex differences by suppressing hepcidin expression.⁽¹⁵⁾ However, there are conflicting reports regarding how testosterone reduces hepcidin.^(15,16) One model proposed that testosterone decreases hepcidin production by enhancing hepatic EGF receptor (EGFR) signaling and reducing R-SMAD phosphorylation.⁽¹⁵⁾ In a second study, EGF was also implicated in hepcidin suppression; however, EGF did not impact R-SMAD

ARTICLE INFORMATION:

From the ¹Program in Anemia Signaling Research, Division of Nephrology, Program in Membrane Biology, Center for Systems Biology; ²Department of Pathology, Massachusetts General Hospital, Harvard Medical School, Boston, MA.

ADDRESS CORRESPONDENCE AND REPRINT REQUESTS TO:

Chia-Yu Wang, Ph.D.
Massachusetts General Hospital
185 Cambridge St., CPZN-8150

Boston, MA 02114
E-mail: cwang@mgh.harvard.edu
Tel.: +1-617-724-9078

phosphorylation but rather reduced R-SMAD nuclear localization.⁽¹⁷⁾ Finally, a third group proposed that testosterone promotes the association of R-SMADs with the androgen receptor, thereby interfering with R-SMAD binding to the hepcidin promoter.⁽¹⁶⁾ A common thread for all of these studies is crosstalk with the BMP-SMAD pathway; however, a functional role for BMP R-SMADs in hepcidin regulation by testosterone and EGF has not been demonstrated *in vivo*.

Three R-SMADs, SMAD1, SMAD5, and SMAD8, are activated by BMP signals. Recently, we showed that mice with an ablation of both *Smad1* and *Smad5* in hepatocytes (*Smad15;Alb-Cre*⁺) exhibited hepcidin deficiency and iron overload, demonstrating the essential role of SMAD1/5 signaling in hepcidin regulation and systemic iron homeostasis.⁽²⁷⁾ SMAD8 was not initially studied because *SMAD8* knockdown did not impact hepcidin expression in cell culture screening assays.⁽²⁷⁾ However, SMAD1 and SMAD5 were differently active *in vitro* and *in vivo*, likely due to copy number variations in the different model systems.⁽²⁷⁾ Moreover, hepcidin was further suppressed by neutralizing BMP antibodies in *Smad15;Alb-Cre*⁺ mice,⁽²⁷⁾ suggesting the presence of residual BMP-SMAD signaling. Notably, SMAD8 has weaker transcriptional activity than SMAD1/5 and was reported not only to stimulate BMP signaling but also to suppress BMP signaling in some contexts by forming a heterodimer with SMAD1.⁽²⁸⁾

Here, we generated hepatocyte-specific *Smad8* single knockout and *Smad1/5/8* triple knockout mice to investigate whether SMAD8 functions to accelerate or antagonize BMP signaling and hepcidin expression *in vivo*. We also used these mouse models to gain mechanistic insight into how inflammation, testosterone, and EGF regulate hepcidin production as well as the pathogenesis of liver injury in hemochromatosis.

Materials and Methods

ANIMALS

Animal protocols were approved by the Institutional Animal Care and Use Committee at Massachusetts General Hospital (MGH). Hepatocyte conditional *Smad8* single knockout (*Smad8*^{fl/wt}; *Alb-Cre*⁺) mice; *Smad1*, *Smad5*, and *Smad8* triple knockout (*Smad15;Alb-Cre*⁺) mice; *Smad1* and *Smad5* double

knockout (*Smad15;Alb-Cre*⁺) mice; and littermate *Cre*⁻ controls were generated by crossing mice harboring a LoxP-flanked allele of *Smad8* (*Smad8*^{fl/wt}) on a mixed C57BL/6J × CD1 background⁽²⁹⁾ (Medical Research Council) with mice expressing a *Cre* (cyclization recombinase) transgene driven by a hepatocyte-specific albumin (*Alb*) promoter⁽⁵⁾ on a C57BL/6J background (Jackson Laboratory) or previously generated hepatocyte *Smad15;Alb-Cre*⁺ mice,⁽²⁷⁾ as described in Supporting Fig. S1. After weaning, mice were maintained on a Prolab 5P75 Isopro RMH 3000 house diet (380 ppm iron). Where indicated, mice received a low-iron (2–6 ppm; TD.80396), sufficient-iron (48 ppm; TD.80394), or high-iron (2% carbonyl iron; TD.08496) diet (Envigo) for 3–5 weeks. Alternatively, mice received one intraperitoneal dose of 1 mg/kg lipopolysaccharide (LPS; serotype 055:B5; Sigma) in phosphate-buffered saline (PBS), five daily oral doses of 200 mg/kg EGFR inhibitor gefitinib (Selleckchem; ZD1839) in dimethyl sulfoxide (DMSO), or an equivalent volume of vehicle.

RNA ISOLATION AND QUANTITATIVE REVERSE TRANSCRIPTION PCR

RNA was isolated using the QIAshredder and RNeasy Mini Kit (Qiagen). First-strand complementary DNA (cDNA) was synthesized from 1 µg RNA using the High Capacity RNA-to-cDNA Kit (Applied Biosystems). Quantitative reverse transcription PCR (qRT-PCR) was performed using the PowerUp SYBR Green Master Mix on the QuantStudio3 Real-Time PCR system (Applied Biosystems), using primers listed in Supporting Table S1. Relative quantities were determined by the standard curve method. Transcript levels were normalized to ribosomal protein L19 (*Rpl19*) as an internal control.

IRON ANALYSIS, BIOCHEMICAL ASSAYS, AND HEPCIDIN ENZYME-LINKED IMMUNOSORBENT ASSAY

Serum iron and unsaturated iron binding capacity were measured by colorimetric assays (Pointe Scientific) to calculate transferrin saturation according to the manufacturer's instructions. Tissue non-heme iron concentrations (in micrograms per gram wet weight) were determined as described.⁽²⁷⁾ Serum

alanine aminotransferase (ALT) and total bilirubin were measured by the MGH Veterinary Clinical Pathology Laboratory. Liver hydroxyproline (Sigma; MAK008) and malondialdehyde (Abcam; ab118970) were determined by colorimetric assays and serum hepcidin by enzyme-linked immunosorbent assay (ELISA; Intrinsic LifeSciences; HMC-001) according to the manufacturers' instructions.

PRIMARY HEPATOCYTE CULTURE

Primary hepatocytes were isolated and cultured as described.⁽²⁷⁾ Where indicated, cells were treated with 20 ng/mL mouse EGF (R&D Systems; 2028-EG) in serum-free growth medium for 24 hours, 100 nM LDN-193189 (Sigma; SML0559) in 2% 2-hydroxypropyl- β -cyclodextrin (Sigma; H107) in 10% fetal bovine serum (FBS) growth medium for 24 hours, or 1% FBS starvation overnight followed by 2 ng/mL mouse IL-6 (R&D Systems; 406-ML) in 1% FBS growth medium for 6 hours.

HISTOLOGY

Tissues were fixed in 10% formalin for 24 hours, embedded in paraffin, sectioned at 6 μ m, and stained for ferric iron (blue) using an iron stain kit with nuclear fast red counterstain according to the manufacturer's instructions (American MasterTech; KTIRO). Collagen was stained for 1 hour using picosirius red solution (0.1% direct red 80 [Sigma; 365548] in 1.3% saturated picric acid [Sigma; P6744]) after 8-minute hematoxylin nuclei staining. Slides were washed with 0.5% acetic acid twice before dehydration and mounting. Images were acquired using a Zeiss LSM 800 Airyscan confocal microscope. Sirius red positivity was quantitated using ImageJ (National Institutes of Health) by dividing the total area calculated under polarized light (after subtracting major veins) by the total area calculated under brightfield.

IMMUNOBLOT

Liver lysates were prepared and immunoblots performed as described⁽²⁷⁾ using rabbit antiphosphorylated EGFR (1:500; Cell Signaling; 2234S), rabbit anti-EGFR (1:1000; Cell Signaling; 4267S), rabbit antiphosphorylated SMAD5 (1:500; Abcam; ab92698), rabbit anti-SMAD5 (1:1000; Abcam; ab40771), or

mouse antiactin (1:20,000; Millipore; MAB1501) antibodies. Chemiluminescence quantification of scanned films was performed using ImageJ 1.46v.

STATISTICS

Data are presented as scatter plots or box plots. Means were compared by Student paired or unpaired *t* test or one-way or two-way analysis of variance (ANOVA) with Tukey's *post hoc* test using Prism 7 (GraphPad). Data with unequal variances were log-transformed prior to statistical analysis. *P* < 0.05 was considered significant.

Results

LIVER *Smad8* mRNA EXPRESSION IS REGULATED BY DIETARY IRON IN WILD-TYPE MICE

Because SMAD8 is positively regulated by BMP signaling *in vitro*⁽²⁷⁾ and liver BMP signaling is regulated by dietary iron in mice,⁽³⁰⁾ we examined the effects of a low-iron (2–6 ppm), sufficient-iron (48 ppm) or high-iron (2% carbonyl) diet on *Smad8* mRNA expression in C57BL/6 wild-type male mice. Mice fed a high-iron diet had a 5-fold increase, whereas mice fed a low-iron diet had a 45% reduction, in *Smad8* mRNA levels compared to mice on an iron-sufficient diet (control, Fig. 1A).

HEPCIDIN EXPRESSION AND IRON LEVELS ARE NOT CHANGED IN HEPATOCYTE *Smad8*^{fl/fl}; *Alb-Cre*⁺ SINGLE-KNOCKOUT MICE

Next, we generated mice with a conditional knock-out of hepatocyte *Smad8* to determine its functional role in hepcidin regulation and iron homeostasis *in vivo*. Excision of LoxP-flanked *Smad8* was confirmed by PCR of total liver genomic DNA (Fig. 1B). qRT-PCR demonstrated >95% lower total liver *Smad8* mRNA levels in *Smad8*^{fl/fl}; *Alb-Cre*⁺ compared with *Cre*⁻ mice (Fig. 1C). Serum iron, serum transferrin saturation, liver iron, and liver hepcidin (hepcidin antimicrobial peptide [*Hamp*]) mRNA levels were unchanged in 8-week-old *Smad8*^{fl/fl}; *Alb-Cre*⁺

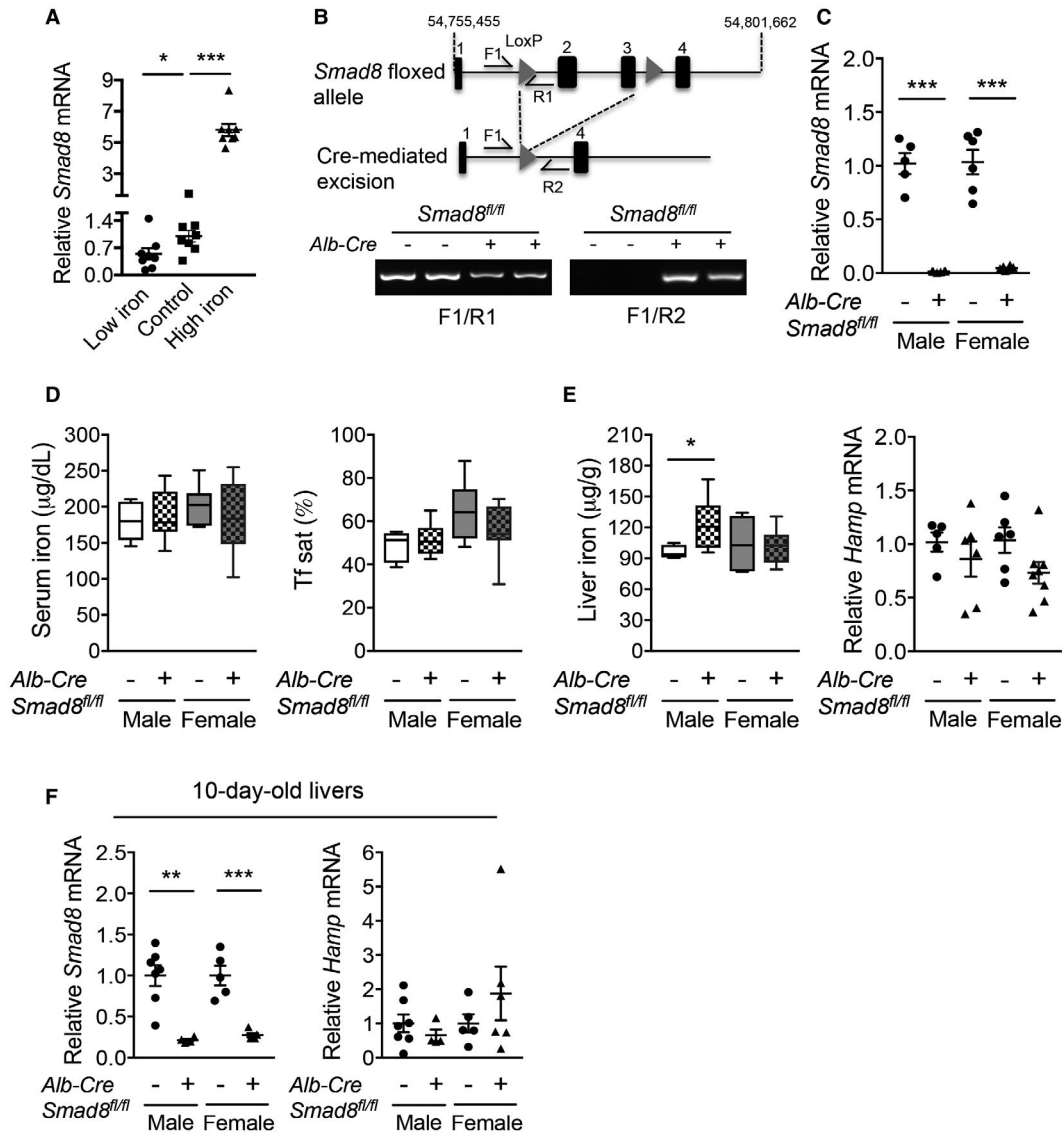


FIG. 1. Iron regulates liver *Smad8* expression, but hepatocyte *Smad8* conditional knockout mice (*Smad8*^{f/f}; *Alb-Cre*⁺) exhibit minimal to no iron loading. (A) Relative *Smad8* expression was measured by quantitative reverse transcription PCR (qRT-PCR) in livers of 7-week-old C57BL/6 male mice after receiving a low-iron (2–6 ppm), sufficient-iron (48 ppm; control), or high-iron (2% carbonyl) diet for 3 weeks (n = 8 per group). (B, top) Schematic depictions of the lox-P-flanked (floxed) *Smad8* allele and the allele after Cre recombinase-mediated excision. F and R indicate forward and reverse primers used for PCR genotyping. (B, bottom) PCR analysis of genomic DNA extracted from total liver of *Smad8*^{f/f}; *Alb-Cre*⁺ mice and littermate *Cre*⁻ controls at 8 weeks of age. (C) Relative *Smad8* mRNA levels in the total livers of *Smad8*^{f/f}; *Alb-Cre*⁺ mice and littermate *Cre*⁻ controls was measured by qRT-PCR to confirm hepatocyte *Smad8* ablation in conditional knockout mice (n = 5–8 per group). (D) Serum iron (left), transferrin saturation (Tf sat; right), (E) hepatic nonheme iron concentrations (left), and liver hepcidin (*Hamp*) expression (right) were quantified in 8-week-old male and female *Smad8*^{f/f}; *Alb-Cre*⁺ mice compared with their respective littermate *Cre*⁻ controls (n = 5–8 per group). (F) Liver *Smad8* and *Hamp* mRNA were measured by qRT-PCR in male and female *Smad8*^{f/f}; *Alb-Cre*⁺ mice and littermate *Cre*⁻ controls at 10 days of age (n = 4–7 per group). All transcript levels were normalized to *Rpl19*, and the average of the respective littermate *Cre*⁻ control mice was set to 1. Data are presented as scatter plots with mean ± SEM or box plots with minimum to maximum whiskers. **P* < 0.05, ***P* < 0.01, ****P* < 0.001 relative to mice fed an iron-sufficient diet by one-way ANOVA with Tukey's *post hoc* test or to the respective *Cre*⁻ controls by Student *t* test.

compared with *Cre*⁻ mice, with the exception of a subtle increase in liver iron in *Smad8*^{f/f}; *Alb-Cre*⁺ male mice (Fig. 1D,E).

We previously reported a similar phenotype of minimal to no iron overload with unchanged *Hamp* expression in 8-week-old hepatocyte single *Smad1* (*Smad1*^{f/f};

Alb-Cre⁺) and *Smad5* (*Smad5^{fl/fl};Alb-Cre⁺*) knockout mice⁽²⁷⁾; however, hepcidin levels were significantly lower in both *Cre⁺* mouse strains compared with *Cre⁻* controls before weaning and in primary hepatocyte cultures, when not exposed to the hepcidin stimulatory effect of the standard rodent diet.⁽²⁷⁾ In contrast, *Hamp* mRNA did not differ in primary hepatocytes (Supporting Fig. S2) or 10-day-old *Smad8^{fl/fl};Alb-Cre⁺* mouse livers (Fig. 1F) compared with *Cre⁻* mice. Moreover, hepcidin expression and serum and tissue iron loading were similarly increased in *Smad8^{fl/fl};Alb-Cre⁺* and *Cre⁻* mice fed a high-iron diet (Supporting Fig. S3). Together, these data suggest that whereas SMAD1 and SMAD5 contribute to basal hepcidin expression, SMAD8 is dispensable for both basal and iron-induced hepcidin expression when SMAD1 and SMAD5 are present. Notably, basal *Smad8* expression was 30-fold and 3-fold lower than *Smad1* and *Smad5*, respectively, by quantitative copy number analysis in mouse hepatocytes (Supporting Fig. S4).

HEPATOCYTE *Smad158;Alb-Cre⁺* TRIPLE KNOCKOUT MICE HAVE MORE SEVERE IRON OVERLOAD THAN *Smad15;Alb-Cre⁺* DOUBLE KNOCKOUT MICE

To investigate how SMAD8 functions in the absence of SMAD1 and SMAD5, we generated littermate hepatocyte *Smad158;Alb-Cre⁺* triple knockout and *Smad15;Alb-Cre⁺* double knockout mice on the same genetic background. qRT-PCR demonstrated that total liver *Smad1* and *Smad5* mRNA levels were equally reduced (>70%) in both *Smad15;Alb-Cre⁺* and *Smad158;Alb-Cre⁺* compared with *Cre⁻* controls (Supporting Fig. S5A,B). As reported,⁽²⁷⁾ liver *Smad8* mRNA was modestly reduced (~50%) in *Smad15;Alb-Cre⁺* mice, most likely due to the regulation of SMAD8 by SMAD1/5 signaling, but was greatly reduced (~95%) in *Smad158;Alb-Cre⁺* mice (Supporting Fig. S5C). All *Cre⁺* mice exhibited high serum iron, transferrin saturation, and liver iron loading and low *Hamp* mRNA levels relative to liver iron content compared with *Cre⁻* controls (Fig. 2A-E). However, serum and liver iron were significantly higher in sex-matched *Smad158;Alb-Cre⁺* compared with *Smad15;Alb-Cre⁺* mice (Fig. 2A,C). Moreover, basal liver *Hamp* expression and *Hamp* mRNA relative

to liver iron content were both significantly lower in *Smad158;Alb-Cre⁺* compared with *Smad15;Alb-Cre⁺* male mice, with a similar trend in female mice (Fig. 2D,E). Additionally, *Smad158;Alb-Cre⁺* mice exhibited significant extrahepatic iron loading in pancreas and heart that began as early as 5 weeks (Supporting Fig. S6) and progressed at 8 weeks of age (Fig. 3A-C). In contrast, no significant extrahepatic iron loading was seen in 8-week-old *Smad15;Alb-Cre⁺* mice on a house diet (Fig. 3A-C), although extrahepatic iron loading could be induced by a high-iron diet (Supporting Fig. S7). Finally, spleen iron was more dramatically reduced in *Smad158;Alb-Cre⁺* mice compared with *Smad15;Alb-Cre⁺* mice (Fig. 3D). Thus, SMAD8 has an important functional role in hepcidin and iron homeostasis regulation in the absence of SMAD1 and SMAD5.

HEPCIDIN DEFICIENCY AND EXTRAHEPATIC IRON LOADING ARE NOT GREATER IN *Smad15;Alb-Cre⁺* AND *Smad158;Alb-Cre⁺* MALE COMPARED TO FEMALE MICE

Prior studies reported that wild-type male mice exhibited lower hepcidin expression than female mice and that lower hepcidin engendered greater extrahepatic iron loading in male compared with female *Bmp6*, *Bmp2*, and *Hjv* global or conditional knockout mice.^(5,6,15,26) We therefore compared hepcidin and iron homeostasis parameters in male versus female *Smad15;Alb-Cre⁺* and *Smad158;Alb-Cre⁺* mice. As reported for wild-type mice,⁽¹⁵⁾ basal *Hamp* mRNA was lower in male compared with female *Cre⁻* mice (Supporting Fig. S8). However, when normalized to liver iron, *Hamp* mRNA was not lower in *Smad15;Alb-Cre⁺* or *Smad158;Alb-Cre⁺* male compared with female mice of the same genotype and, in fact, was lower in *Smad15;Alb-Cre⁺* female than male mice (Fig. 2E). Moreover, liver iron levels were higher in both *Cre⁺* female compared with genotype-matched male mice, and serum iron was higher in *Smad158;Alb-Cre⁺* female mice (Fig. 2A,C). Finally, although extrahepatic iron loading was not seen in 8-week-old *Smad15;Alb-Cre⁺* mice, *Smad158;Alb-Cre⁺* female mice exhibited similar or greater extrahepatic iron loading as male mice (Fig. 3A-C; Supporting Fig. S6B,C).

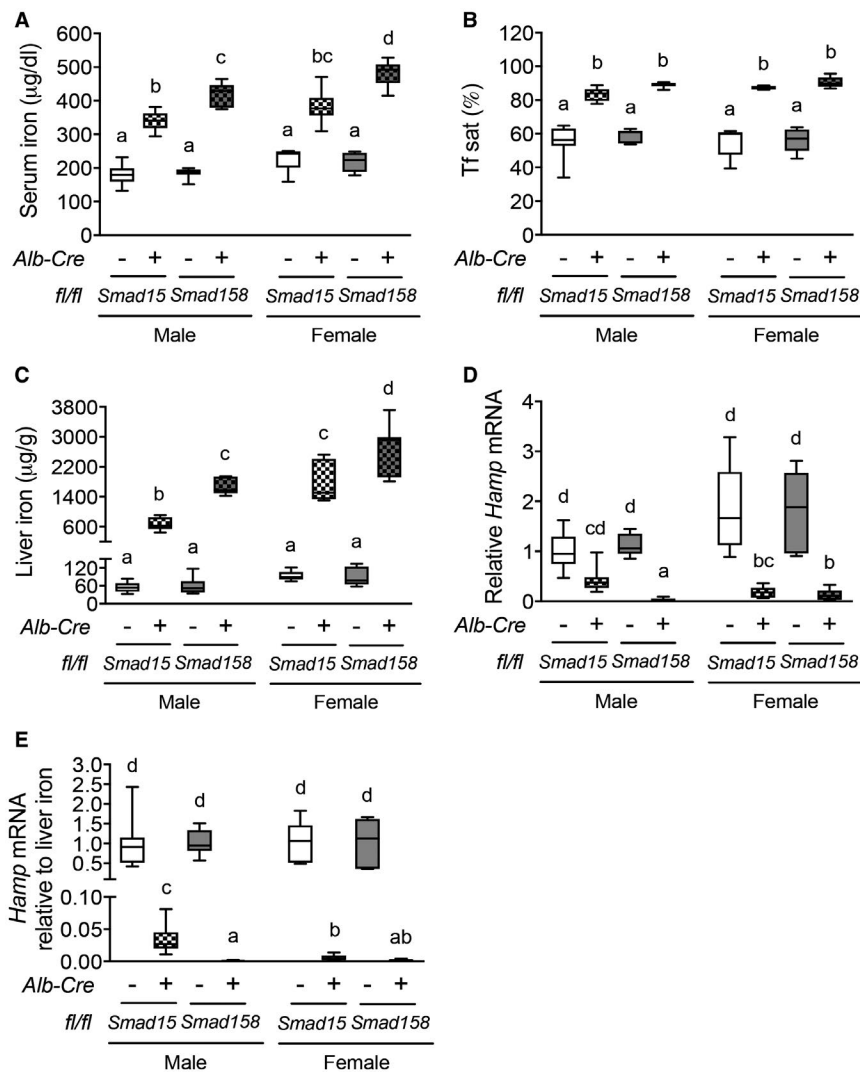


FIG. 2. Smad1/5/8 triple knockout mice (*Smad158;Alb-Cre*⁺) exhibit more severe hepcidin deficiency and iron overload compared with Smad1/5 double knockout mice (*Smad15;Alb-Cre*⁺). (A) Serum iron, (B) Tf sat, (C) liver iron concentration, (D) liver *Hamp* mRNA, and (E) liver *Hamp* mRNA levels relative to liver iron concentration were measured in 8-week-old male and female *Smad15;Alb-Cre*⁺ and *Smad158;Alb-Cre*⁺ mice and their respective littermate *Cre*⁻ controls (n = 5–8 per group). Transcript levels were normalized to *Rpl19*, and the average of male *Smad15;Alb-Cre*⁻ control mice was set to 1. Data are presented as box plots with minimum to maximum whiskers. Results were compared across genotype and sex by two-way ANOVA with Tukey's *post hoc* test. Means without a common superscript differ significantly ($P < 0.05$).

EGFR INHIBITION DOES NOT INCREASE HEPCIDIN IN MALE MICE

Testosterone-mediated hepcidin suppression was demonstrated to account for the sexual dimorphism in wild-type and *Bmp6* knockout mice.^(15,16) In one study, activation of EGFR signaling and suppression of SMAD5 phosphorylation⁽¹⁵⁾ were proposed

as mechanisms. Consistent with the prior study,⁽¹⁵⁾ male *Smad15;Alb-Cre*⁺ and *Smad158;Alb-Cre*⁺ mice had increased *Egfr* mRNA compared to genotype-matched female mice (Fig. 4A). However, in contrast to the prior report,⁽¹⁵⁾ although administration of the EGFR inhibitor gefitinib reduced EGFR phosphorylation (Fig. 4B), gefitinib did not increase *Hamp* mRNA or SMAD5 phosphorylation in wild-type male mice (Fig. 4C,D). Thus, although the absence

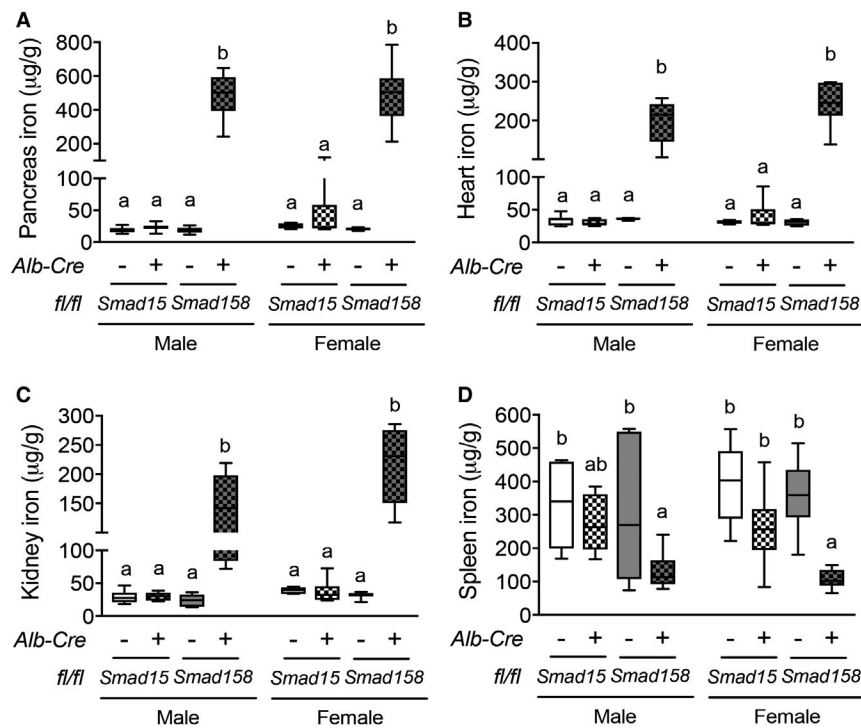


FIG. 3. Eight-week-old *Smad158;Alb-Cre⁺*, but not *Smad15;Alb-Cre⁺*, mice exhibit extrahepatic iron loading in pancreas, heart, and kidney with similar severity in female and male mice. Eight-week-old male and female *Smad15;Alb-Cre⁺* and *Smad158;Alb-Cre⁺* mice and their respective littermate *Cre⁻* controls were analyzed for tissue iron in (A) pancreas, (B) heart, (C) kidney, and (D) spleen (n = 5–8 per group). Data are presented in box plots with minimum to maximum whiskers. Results were compared across genotype and sex by two-way ANOVA with Tukey's *post hoc* test. Means without a common superscript differ significantly ($P < 0.05$).

of more severe hepcidin deficiency and extrahepatic iron loading in *Smad15;Alb-Cre⁺* and *Smad158;Alb-Cre⁺* male mice compared with female mice provides *in vivo* evidence for a critical functional role for BMP R-SMADs in hepcidin suppression by testosterone, we could not confirm a functional role for EGFR signaling in testosterone-mediated hepcidin suppression.

EGF FAILS TO SUPPRESS HEPCIDIN IN *Smad15;Alb-Cre⁺* HEPATOCYTES

Although our data suggest that EGFR signaling is not involved in testosterone-mediated hepcidin suppression, EGF itself has been demonstrated to suppress hepcidin expression.⁽¹⁷⁾ To determine whether hepcidin suppression by EGF requires BMP R-SMAD signaling, we tested whether EGF reduced *Hamp* expression in *Smad15;Alb-Cre⁺* primary hepatocytes that have a residual capacity for hepcidin suppression (Fig. 2D), which we

confirmed *in vitro* using the BMP type I receptor inhibitor LDN-193189⁽²¹⁾ treatment (Fig. 4E). Whereas EGF suppressed *Hamp* mRNA in *Cre⁻* primary hepatocytes, it did not suppress *Hamp* mRNA in *Smad15;Alb-Cre⁺* hepatocytes (Fig. 4F). Collectively, these data provide functional evidence that SMAD1/5 signaling is required for hepcidin suppression by EGF, at least *in vitro*.

LPS INDUCES HEPCIDIN PRODUCTION IN *Smad158;Alb-Cre⁺* MICE

IL-6 plays a key role in hepcidin induction by inflammation.⁽¹²⁾ To investigate whether IL-6-mediated hepcidin induction requires BMP R-SMADs, we tested the effects of LPS injection in *Smad158;Alb-Cre⁺* mice versus *Cre⁻* controls. LPS significantly induced endogenous liver *Il6* mRNA in both genotypes after 6 hours (Fig. 5A). In *Cre⁻* mice, LPS also increased liver *Smad1* and *Smad5* but suppressed *Smad8* mRNA

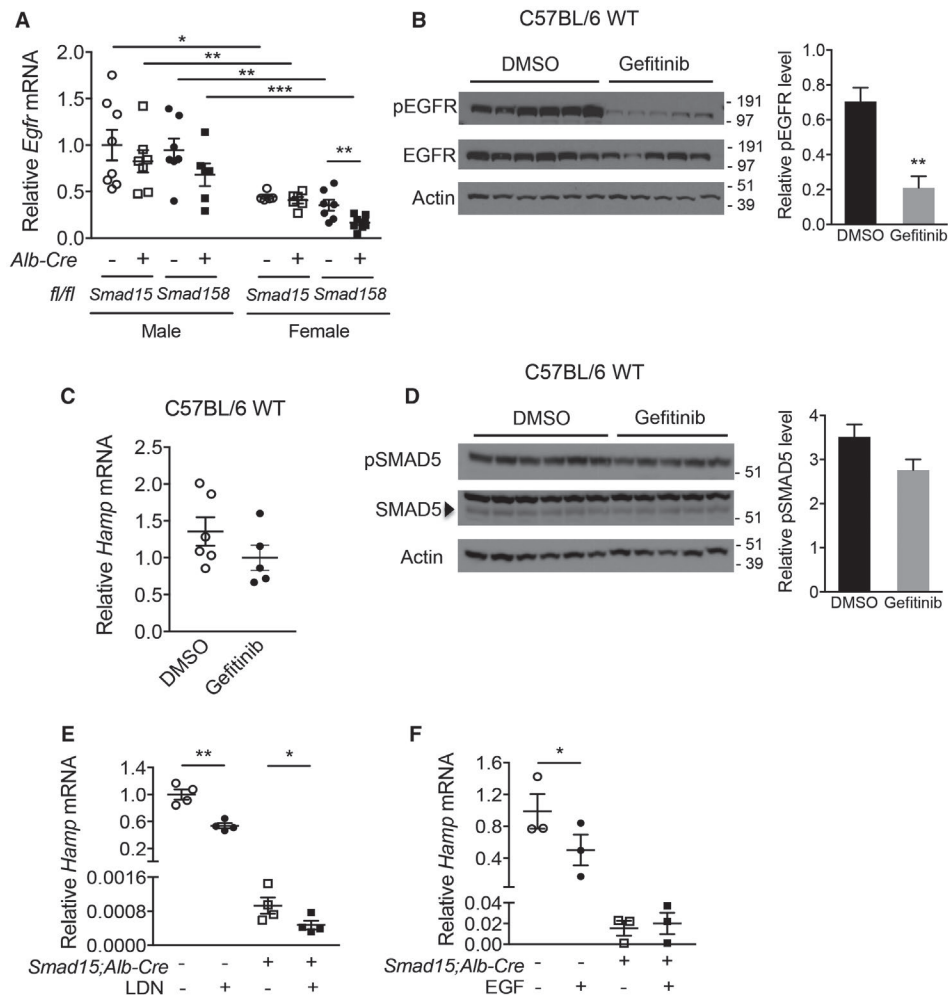


FIG. 4. The EGFR inhibitor gefitinib does not reverse hepcidin suppression in male mice, but hepatocyte ablation of *Smad1* and *Smad5* abolishes hepcidin suppression by EGF. (A) Eight-week-old male and female *Smad15;Alb-Cre*⁺ and *Smad158;Alb-Cre*⁺ mice and their respective littermate *Cre*⁻ controls were analyzed for hepatic *Egfr* mRNA (n = 5-8 per group). (B-D) C57BL/6 wild-type male mice at 7 weeks were treated with 200 mg/kg gefitinib or DMSO vehicle by oral gavage for 5 days (n = 5-6 per group). Mice were sacrificed 6 hours after the final dose, and livers were analyzed for (B) EGFR phosphorylation and (D) SMAD5 phosphorylation levels by immunoblot and chemiluminescence quantitation and (C) *Hamp* mRNA by qRT-PCR. (E,F) Primary hepatocytes were isolated from 7-week-old *Smad15;Alb-Cre*⁺ and littermate *Cre*⁻ control mice. Hepatocyte *Hamp* mRNA was analyzed by qRT-PCR in cells treated with (E) 100 nM LDN-193189 in 2% 2-hydroxypropyl- β -cyclodextrin or (F) 20 ng/mL mouse recombinant EGF or vehicle alone for 24 hours. Data from four (E) or three (F) independent experiments, each performed in triplicate, are shown. Transcripts were normalized to *Rpl19*, and the average of male *Smad15;Alb-Cre*⁻ or vehicle-treated *Cre*⁻ control mice were set to 1. Data are presented in scatter plots with mean \pm SEM. **P* < 0.05, ***P* < 0.01, ****P* < 0.001 relative to female mice or vehicle-treated control mice of the same genotype or as otherwise noted by Student *t* test. Abbreviation: LDN, LDN-193189.

(Fig. 5B,C). Liver *Hamp* mRNA and serum hepcidin were significantly increased by LPS in both genotypes (Fig. 5D,E). The fold-induction in *Hamp* mRNA was similar or greater in *Cre*⁺ compared to *Cre*⁻ mice, although the fold-induction in serum hepcidin was less, and lower baseline hepcidin resulted in lower peak hepcidin levels in *Cre*⁺ mice. Because LPS also

induces inflammatory cytokines other than IL-6, we also measured *Hamp* mRNA in primary hepatocytes treated with IL-6 and found similar results (Fig. 5F). These data suggest that IL-6 still induces hepcidin in the absence of BMP R-SMADs, although R-SMADs do influence the absolute levels of hepcidin achieved by altering the basal setpoint.

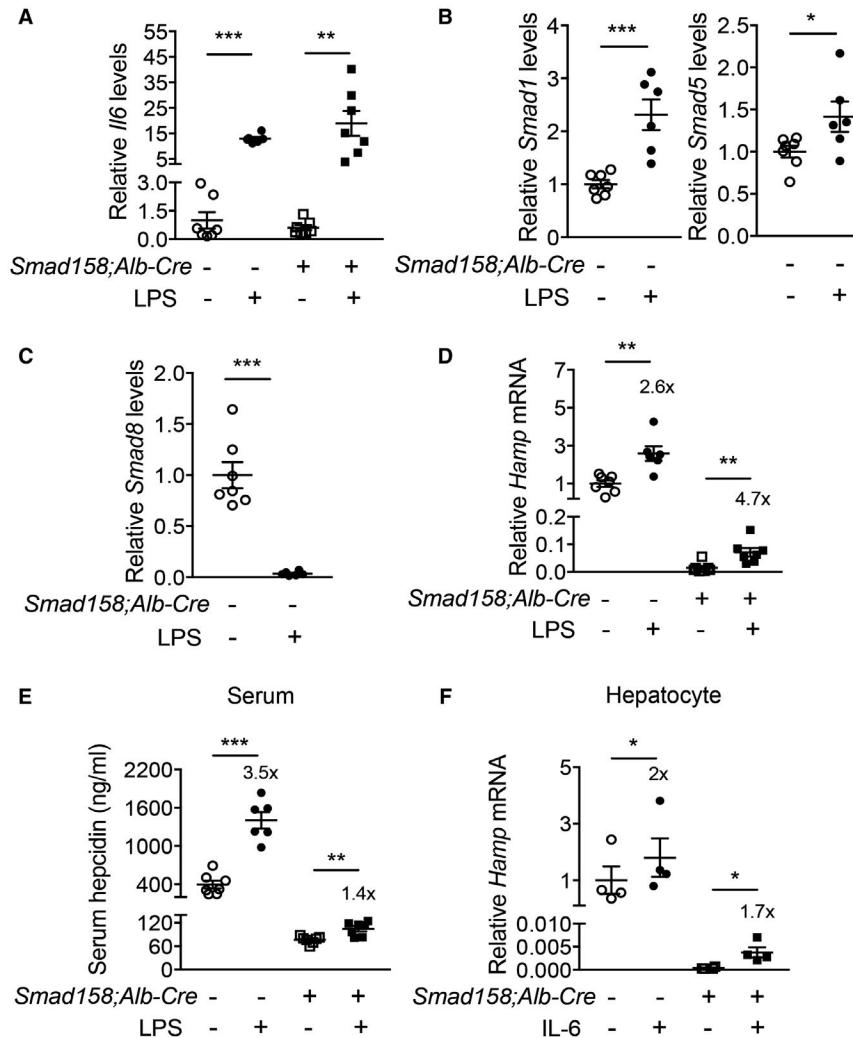


FIG. 5. Inflammation significantly increases hepcidin production in *Smad158;Alb-Cre*⁺ mice. Male and female *Smad158;Alb-Cre*⁺ and littermate *Cre*⁻ control mice (n = 6-7 per group) at 6 weeks of age were injected with PBS or LPS (1 mg/kg body weight) and sacrificed after 6 hours. Livers and serum were collected to determine (A) *Il6*, (B) *Smad1/5*, (C) *Smad8*, (D) *Hamp* mRNA expression by qRT-PCR, and (E) serum hepcidin protein levels by ELISA. (F) Primary hepatocytes isolated from 6-week-old *Smad158;Alb-Cre*⁺ and littermate *Cre*⁻ control mice (n = 4 per group) were treated with 2 ng/mL IL-6 for 6 hours and *Hamp* mRNA levels were determined. Data from four independent experiments, each performed in triplicate, are shown. Transcripts were normalized to *Rpl19* and the average of PBS-treated *Cre*⁻ control mice were set to 1. Data are presented as scatter plots with mean ± SEM. **P* < 0.05, ***P* < 0.01, ****P* < 0.001 relative to PBS-treated controls of the same genotype by Student *t* test. Fold-change relative to PBS treatment for each genotype are reported in (D-F).

Smad1/5/8;Alb-Cre⁺ MICE EXHIBIT LIVER TISSUE INJURY AND FIBROSIS AT 8 WEEKS

Tissue iron accumulation in human hemochromatosis patients leads to injury and organ dysfunction.⁽³⁾ Although mouse models of hemochromatosis phenocopy the iron overload seen in humans, most

mouse models do not develop tissue injury and fibrosis.⁽³¹⁻³⁴⁾ The severity of liver iron accumulation in *Smad158;Alb-Cre*⁺ mice led us to examine for evidence of liver damage and fibrosis. Eight-week-old male and female *Smad158;Alb-Cre*⁺ mice exhibited a significant increase in serum ALT (3 to 6-fold) and total bilirubin compared to *Cre*⁻ controls, consistent with liver injury (Fig. 6A,B). Liver malondialdehyde

was also increased, indicative of oxidative stress and lipid peroxidation (Fig. 6C). Histologic analysis (Fig. 6D,E; Supporting Figs. S9 and S10) showed scattered apoptotic hepatocytes, confirmed by terminal deoxynucleotidyl transferase–mediated deoxyuridine triphosphate nick-end labeling (TUNEL) staining, and numerous ceroid-laden macrophages (which have phagocytosed dead hepatocytes), predominantly in the centrilobular (zone 3) region. Hepatocyte mitotic figures were also present, indicative of response to injury. Occasional foci of mononuclear inflammation were present in zone 3, but overall inflammation was mild. These changes were not observed in *Cre*⁻ controls. Prussian blue staining showed marked hepatocytic iron deposition as well as positive staining of ceroid-laden macrophages in zone 3 in *Smad158;Alb-Cre*⁺ mice but not *Cre*⁻ mice. Because there was no visible iron staining in sinusoidal Kupffer cells, the iron in ceroid-laden macrophages likely reflects iron originally deposited in damaged, phagocytosed hepatocytes. Picrosirius red staining showed sinusoidal/pericellular fibrosis in zone 3 in the *Smad158;Alb-Cre*⁺ mice (5 to 6-fold higher than *Cre*⁻ mice), indicating chronic injury to hepatocytes. Additional indicators of liver fibrosis, collagen type I alpha 1 (*Col1a1*) mRNA and hydroxyproline, were also increased in *Smad158;Alb-Cre*⁺ mice compared to *Cre*⁻ controls (Fig. 6F). Collectively, the histopathologic findings in *Smad158;Alb-Cre*⁺ mice reveal hepatocytic iron deposition, accompanied by active and chronic hepatocyte injury in a predominantly zone 3 distribution. In contrast to the liver, we did not find biochemical or histologic evidence of injury in the pancreas or heart of *Smad158;Alb-Cre*⁺ mice, despite iron loading (Supporting Figs. S11 and S12).

HEPATIC IRON LOADING AND SMAD1/5/8 DEFICIENCY BOTH CONTRIBUTE TO LIVER INJURY AND FIBROSIS IN *Smad158;Alb-Cre*⁺ MICE

To investigate the cause(s) of liver injury and fibrosis in *Smad158;Alb-Cre*⁺ mice, we examined liver injury parameters and histology in 8-week-old *Smad15;Alb-Cre*⁺ mice versus *Cre*⁻ controls. Serum ALT was 3-fold higher in *Smad15;Alb-Cre*⁺ female mice compared with *Cre*⁻ controls with some features

of liver injury by histologic analysis, although picrosirius red quantitation and *Col1a1* mRNA levels were not significantly increased due to large animal-to-animal variability (Supporting Fig. S13). Serum ALT, liver *Col1a1* mRNA, and picrosirius red were significantly increased in both male and female *Smad15;Alb-Cre*⁺ mice fed a high-iron diet (Supporting Fig. S13). Thus, *Smad8* deletion *per se* is not required for liver injury.

Notably, the degree of liver injury and fibrosis in *Cre*⁺ mice (Fig. 6; Supporting Fig. S13) paralleled the degree of liver iron loading, which was most severe in *Smad158;Alb-Cre*⁺ female mice, followed by *Smad158;Alb-Cre*⁺ male and *Smad15;Alb-Cre*⁺ female mice, followed by *Smad15;Alb-Cre*⁺ male mice (Fig. 2C). Moreover, serum ALT was only modestly increased in female mice, and *Col1a1* mRNA was not increased in 5-week-old *Smad158;Alb-Cre*⁺ mice whose livers were less iron-loaded (Supporting Fig. S6) than 8-week-old *Smad158;Alb-Cre*⁺ mice. To confirm whether iron loading plays a pathogenic role in liver injury and fibrosis, we evaluated *Smad158;Alb-Cre*⁺ mice and *Cre*⁻ controls maintained on a low-iron diet between 4 and 8 weeks of age to minimize liver iron loading. Although serum and liver iron levels were still higher in low-iron diet *Smad158;Alb-Cre*⁺ mice compared with *Cre*⁻ controls (Fig. 7A-C) in the context of hepcidin deficiency (Fig. 7D), liver iron levels were much lower in *Smad158;Alb-Cre*⁺ mice on a low-iron diet (~200 µg/g; Fig. 7C) compared with a house diet (~2,200 µg/g; Fig. 2C). Importantly, serum ALT and liver *Col1a1* mRNA were not increased in low-iron diet *Smad158;Alb-Cre*⁺ mice compared to *Cre*⁻ mice (Fig. 7E,F).

To explore whether a deficiency in SMAD1/5/8 signaling also contributes to liver injury and fibrosis, 3-week-old *Cre*⁻ control mice received a high-iron diet for 5 weeks to induce serum and liver iron loading to similar levels as *Smad158;Alb-Cre*⁺ mice on a house diet (Fig. 8A). As expected, *Hamp* mRNA was increased in *Cre*⁻ mice fed a high-iron diet compared to both *Cre*⁻ and *Cre*⁺ mice on a house diet (Fig. 8B). Interestingly, despite similar liver iron loading, serum ALT, liver *Col1a1* mRNA, liver picrosirius red staining, and other histologic evidence of hepatocyte injury were significantly reduced in high-iron diet *Cre*⁻ female mice compared to house-diet *Smad158;Alb-Cre*⁺ female mice, with similar trends seen in male mice (Fig. 8C-F). Collectively, these

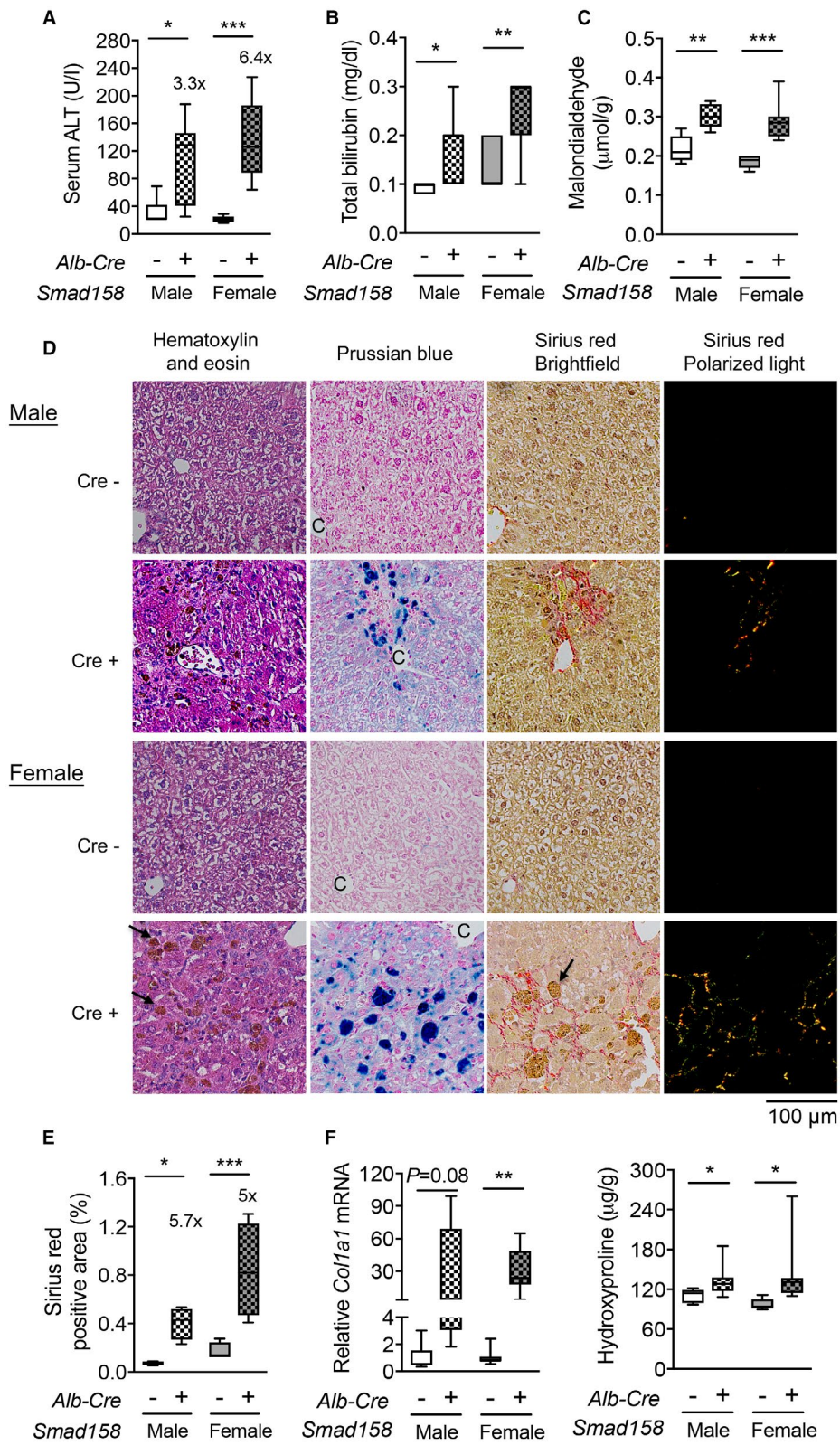


FIG. 6. *Smad158;Alb-Cre⁺* mice develop liver injury and fibrosis at 8 weeks of age. Male and female *Smad158;Alb-Cre⁺* and littermate *Cre⁻* control mice were sacrificed at 8 weeks of age (n = 6–8 per group). Serum was collected to measure (A) ALT and (B) total bilirubin. (C,F) Liver malondialdehyde, hydroxyproline, and *Col1a1* relative to *Rpl19* mRNA levels were quantified by colorimetric assays or qRT-PCR. (D) Liver sections from a subset of mice (n = 4 per group) were stained with hematoxylin and eosin, Perls' Prussian blue for tissue iron, or picrosirius red for collagen formation. Branches of the central vein (C) and ceroid-laden macrophages (arrows) are indicated. Images were taken under brightfield and/or polarized light, and representative images are shown. (E) The sirius red-positive area was quantitated by dividing total area calculated in polarized light (after subtraction of major veins) by total area calculated under brightfield (n = 4 per group). Data are presented as box plots with minimum to maximum whiskers. For qRT-PCR, the average of male *Cre⁻* control mice was set to 1. **P* < 0.05, ***P* < 0.01, ****P* < 0.001 relative to their respective *Cre⁻* controls by Student *t* test.

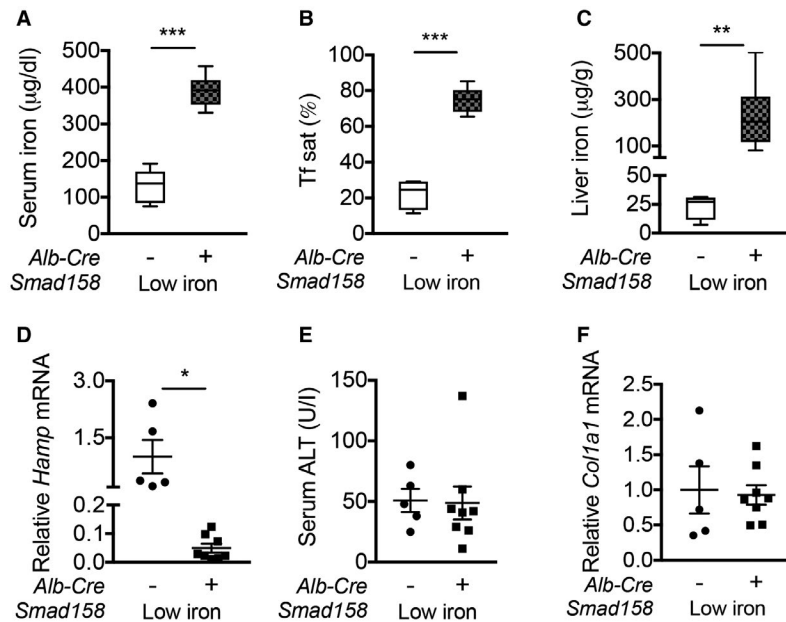


FIG. 7. A low-iron diet prevents liver injury and fibrosis in *Smad158;Alb-Cre⁺* mice. Four-week-old male and female *Smad158;Alb-Cre⁺* and littermate *Cre⁻* control mice were treated with a low-iron diet for 4 weeks (n = 5–8 per group). At 8 weeks of age, serum and livers were collected to determine (A) serum iron, (B) serum Tf sat, (C) liver iron, and (E) serum ALT. (D) Liver *Hamp* and (F) liver *Col1a1* mRNA levels were measured by qRT-PCR. Transcript levels were normalized to *Rpl19*, and the average of *Cre⁻* control mice was set to 1. Data are presented as scatter plots with mean ± SEM or box plots with minimum to maximum whiskers. **P* < 0.05, ***P* < 0.01, ****P* < 0.001 relative to *Cre⁻* control mice on a low-iron diet by Student *t* test.

data suggest that hepatocyte *Smad1/5/8* ablation contributes to the development of liver injury and fibrosis in response to iron loading.

Discussion

BMP R-SMADs are major transcriptional regulators of hepcidin that govern systemic iron homeostasis⁽⁴⁾; however, the relative contribution of SMAD1, SMAD5, and SMAD8 has been uncertain. We recently demonstrated that SMAD1 and SMAD5 have critical but redundant and dose-dependent roles in hepcidin and iron homeostasis regulation because

hepatocyte ablation of both *Smad1* and *Smad5* in mice resulted in hepcidin deficiency and iron overload, whereas ablation of either *Smad1* or *Smad5* reduced basal hepcidin levels but only marginally impacted iron-dependent and BMP-dependent hepcidin induction.⁽²⁷⁾ Here, we demonstrated that, unlike SMAD1 or SMAD5, SMAD8 is dispensable for basal hepcidin expression because hepcidin levels were unchanged in *Smad8^{fl/fl};Alb-Cre⁺* mice. Although liver *Smad8* expression was regulated by dietary iron, *Smad8^{fl/fl};Alb-Cre⁺* mice responded appropriately to a dietary iron challenge. This dispensability of SMAD8 in the presence of SMAD1 and SMAD5 may be due to the lower expression of *Smad8* compared with *Smad1* and *Smad5*

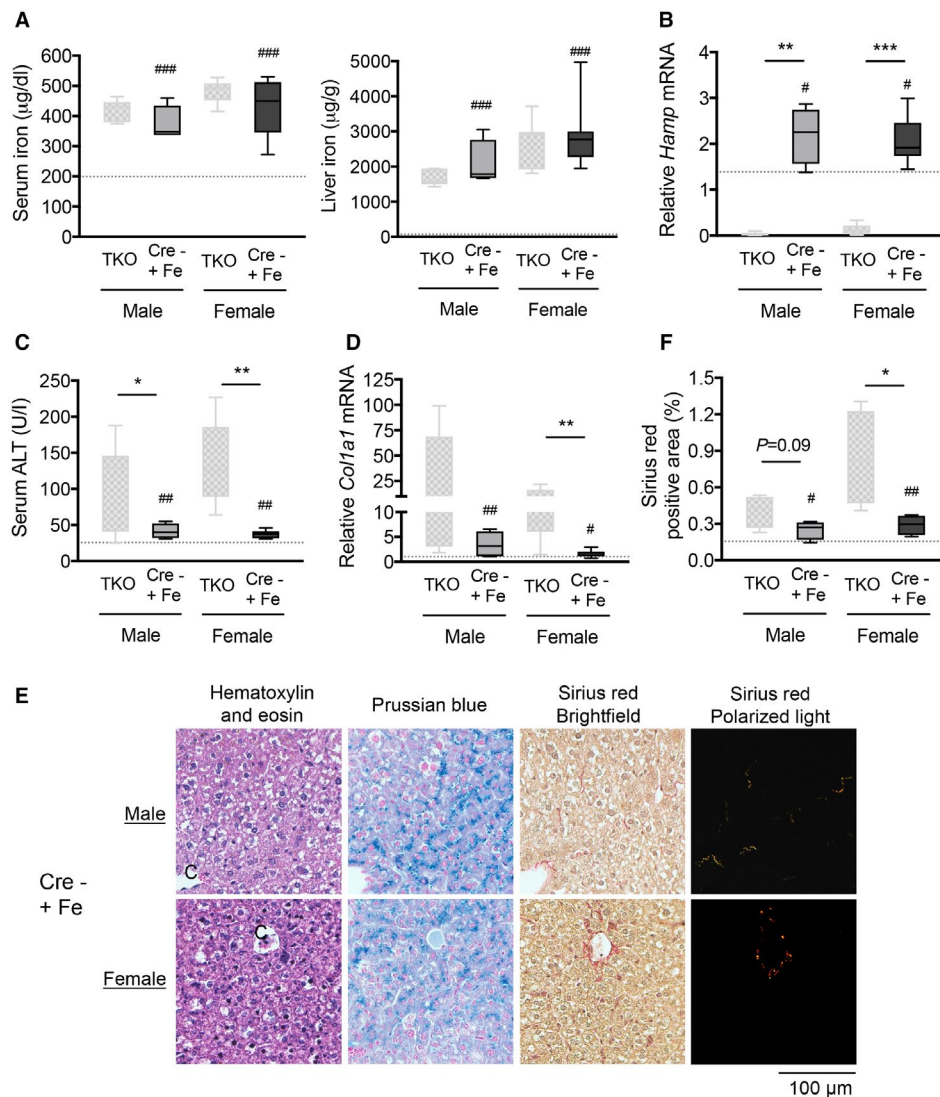


FIG. 8. Hepatocyte ablation of *Smad1/5/8* worsens iron-induced liver injury and fibrosis in mice. Three-week-old male and female *Smad15;Alb-Cre⁻* mice were fed a high-iron (2% carbonyl iron) diet for 5 weeks (*Cre⁻* +Fe, n = 4–8 per group). At 8 weeks of age, tissues were collected to measure (A) serum iron and liver iron and (C) serum ALT. (B) Liver *Hamp* and (D) *Col1a1* relative to *Rpl19* mRNA levels were measured by qRT-PCR. Data are presented as box plots with minimum to maximum whiskers. Results from *Smad158;Alb-Cre⁺* mice on a house diet from Figs. 2 and 6 were replotted for comparison (TKO). Dotted lines represent the average of all *Cre⁻* mice on a house diet from Figs. 2 and 6 for reference. For qRT-PCR, results are normalized to the average of male *Smad158;Alb-Cre⁻* control mice on a house diet, which was set to 1. #*P* < 0.05, ##*P* < 0.01, ###*P* < 0.001 relative to *Cre⁻* mice on a house diet by Student *t* test. **P* < 0.05, ***P* < 0.01, ****P* < 0.001 relative to sex-matched TKO mice by Student *t* test. (E) In a subset of mice (n = 4 per group), liver sections were stained with hematoxylin and eosin, Perl's Prussian blue for tissue iron, or picrosirius red for collagen formation. Images were taken under brightfield and/or polarized light, and representative images are shown. (F) The sirius red-positive area was quantitated by dividing total area calculated in polarized light (after subtraction of major veins) by total area calculated under brightfield (n = 4 per group). Data in (F) are presented and analyzed as in (A–D).

in mouse hepatocytes. SMAD8 was also reported to have reduced transcriptional activity compared with SMAD1 and SMAD5.⁽²⁸⁾ Although not required for hepcidin regulation in the presence of SMAD1 and

SMAD5, SMAD8 does have a critical role in hepcidin transcription in the absence of SMAD1 and SMAD5 because triple knockout *Smad158;Alb-Cre⁺* mice had lower hepcidin expression than double

knockout *Smad15;Alb-Cre⁺* mice. Moreover, lower hepcidin in *Smad158;Alb-Cre⁺* mice was associated with increased iron overload, including the development of extrahepatic iron loading. A similar pattern of lower hepcidin leading to extrahepatic iron overload has been observed in other mouse hemochromatosis models, attributed to a greater or faster accumulation of non-transferrin-bound iron that overwhelms the liver's uptake capacity.^(5,15)

The *Smad158;Alb-Cre⁺* mice provide a model to study the mechanisms of liver injury and fibrosis in hemochromatosis. In contrast to humans,⁽³⁾ liver injury and fibrosis are not reported in most mouse hemochromatosis models.⁽³¹⁻³⁴⁾ For example, no liver injury or fibrosis was reported in mice lacking *Hfe* or *Hjv*, even after a high-iron diet.^(31,34) *Hamp* knockout mice developed ALT elevations only after receiving a high-iron diet for 5 months, and liver fibrosis was not detected until 12 months.⁽³²⁾ *Hfe/Tfr2* double mutant mice were reported to develop ALT elevation and portal fibrosis, but the changes were relatively modest (80% increase in ALT, 3.5-fold increase in collagen) at 11 weeks.⁽³³⁾ There was a brief mention of liver injury and inflammation in 8-month-old hepatocyte *Smad4* knockout mice, but this was poorly characterized.⁽²⁰⁾ In the present study, 8-week-old *Smad158;Alb-Cre⁺* mice were found to have 3-fold to 6-fold higher ALT levels, with a histopathologic correlate of apoptotic hepatocytes, ceroid-laden macrophages, and increased collagen formation compared to *Cre⁻* controls. It is difficult to quantitatively compare the *Smad158;Alb-Cre⁺* mice and other hemochromatosis models because they are on different background strains, which influences iron loading severity,⁽³⁵⁾ and some models are not fully characterized. However, our data suggest that at least two factors contribute to the pathogenesis of liver injury and fibrosis in *Smad158;Alb-Cre⁺* mice. Iron overload is required because liver injury and fibrosis were prevented by a low-iron diet. SMAD1/5/8 deficiency also plays a pathogenic role because *Cre⁻* mice with similar iron overload as *Smad158;Alb-Cre⁺* mice were protected from liver injury and fibrosis. This was not specifically a consequence of *Smad8* deficiency because *Smad15;Alb-Cre⁺* mice also exhibited some degree of liver injury. Notably, *HFE*, *TFR2*, and *HJV* mutations are also associated with reduced hepatic SMAD1/5/8 signaling,^(8-11,36) raising the hypothesis that deficient SMAD1/5/8 signaling could contribute to the pathophysiology of liver disease in human

patients with hereditary hemochromatosis. There were some differences between the pattern of hepatocyte injury and fibrosis in *Smad158;Cre⁺* mice, which was predominantly centrilobular (zone 3), compared with human hemochromatosis patients, where injury and fibrosis typically begin in the portal/periportal region (zone 1) before progressing to bridging zone 1–zone 3 fibrosis and cirrhosis. The explanation for these apparent differences will require additional investigation.

Our study helps to clarify the role of BMP-SMAD1/5/8 signaling in hepcidin induction by inflammation. It was previously proposed that SMAD1/5/8 signaling is required for hepcidin induction by LPS/IL-6 through crosstalk at the receptor and/or intracellular levels because LPS/IL-6 still induced hepcidin in *Bmp6^{-/-}* or *Hjv^{-/-}* mice^(37,38) but failed to induce hepcidin in hepatocyte activin receptor-like kinase 3 (*Alk3*) or *Smad4* knockout mice.^(20,23) However, we demonstrated here that in the absence of hepatocyte *Smad1/5/8*, hepcidin was still induced by LPS *in vivo* and IL-6 *in vitro*. These data demonstrate that BMP R-SMADs are not required for hepcidin induction by LPS/IL-6. The apparent lack of hepcidin induction by IL-6 in the *Alk3* and *Smad4* mice may be due to differences in experimental protocol. Alternatively, there could be signals governed by SMAD1/5/8-independent but ALK3-dependent or SMAD4-dependent pathways. For example, ALK3 can activate non-SMAD pathways and TGF- β and activin ligands require SMAD4 but use SMAD2/3 rather than SMAD1/5/8.⁽³⁹⁾ Although our study was limited by the use of conditional knockout models, we previously demonstrated >99% recombination efficiency with *Alb-Cre*,⁽⁵⁾ and both *Alk3* and *Smad4* mice have the same limitation.^(20,23) Notably, although LPS and IL-6 increased hepcidin in *Smad1/5/8*-deficient hepatocytes, basal hepcidin levels were dramatically lower, resulting in lower peak hepcidin levels. Thus, although not required for hepcidin induction by LPS/IL-6, SMAD1/5/8 does influence final hepcidin levels achieved by altering the basal set point. These data are consistent with the hepcidin-lowering effects reported for BMP-SMAD1/5/8 inhibitors in animal models of anemia of inflammation.^(21,22)

The *Smad158;Alb-Cre⁺* mice have also enabled insights into the mechanisms of hepcidin regulation by testosterone and EGF. Multiple groups demonstrated

that the hepcidin-suppressive effects of testosterone account for lower hepcidin expression in male compared with female mice,^(15,16) and this is proposed to account for the greater extrahepatic iron overload seen in *Bmp6*,^(5,15) *Hjv*,⁽²⁶⁾ and *Bmp2*⁽⁶⁾ global or conditional knockout mice. Here, we demonstrated that hepcidin expression was not lower and extrahepatic iron loading was not increased in male compared with female *Smad15;Alb-Cre*⁺ or *Smad158;Alb-Cre*⁺ mice, providing *in vivo* evidence of a crucial functional role for BMP R-SMADs in hepcidin regulation by testosterone. Interestingly, *Hamp* expression was lower in *Smad15;Alb-Cre*⁺ female compared with male mice, which may be attributed to the hepcidin-suppressive effects of estrogen, which acts directly through an estrogen response element on the hepcidin promoter.^(13,14) Notably, our data did not corroborate one proposed model that testosterone suppresses hepcidin by enhancing EGFR signaling⁽¹⁵⁾ because EGFR inhibition did not reverse hepcidin suppression in male mice in our study. Our data are consistent with another proposed model that testosterone sequesters SMAD1 and SMAD4 with the androgen receptor to reduce their association with the hepcidin promoter,⁽¹⁶⁾ although this requires further validation *in vivo*. These findings may help shed light on some of the sex differences in iron loading and liver disease progression in hemochromatosis patients.

Our data also provide functional evidence of a critical role for BMP R-SMADs in hepcidin suppression by EGF. These findings are consistent with a prior study demonstrating that EGF reduces nuclear localization of BMP R-SMADs in cell culture.⁽¹⁷⁾ Another growth factor, HGF, was also reported to increase expression of the SMAD corepressor TG-interacting factor.⁽¹⁷⁾ Future studies will be needed to understand the relative contribution of these proposed mechanisms *in vivo*. These studies may have implications for developing therapies for chronic liver diseases, where hepcidin suppression by EGF has been postulated to contribute to hepcidin deficiency and iron loading, which correlates with poorer outcomes.^(17,40)

In summary, *Smad158;Alb-Cre*⁺ mice are a model of hemochromatosis that establishes the redundant but critical role for all BMP R-SMADs in hepcidin and iron homeostasis regulation. This model reveals the crucial role of BMP R-SMADs in hepcidin suppression by EGF and the sexual dimorphism reported in some mouse models of hemochromatosis, which

is independent of EGFR signaling. Additionally, although BMP R-SMADs contribute to elevated hepcidin levels in the context of inflammation, this is mainly as a consequence of reducing basal hepcidin levels rather than impacting the IL-6 response. Finally, our data suggest a functional role for SMAD1/5/8 deficiency in liver injury and fibrosis in the context of iron overload.

REFERENCES

- 1) Nemeth E, Tuttle MS, Powelson J, Vaughn MB, Donovan A, Ward DM, et al. Hepcidin regulates cellular iron efflux by binding to ferroportin and inducing its internalization. *Science* 2004;306:2090-2093.
- 2) Roetto A, Papanikolaou G, Politou M, Alberti F, Girelli D, Christakis J, et al. Mutant antimicrobial peptide hepcidin is associated with severe juvenile hemochromatosis. *Nat Genet* 2003;33:21-22.
- 3) Brissot P, Pietrangelo A, Adams PC, de Graaff B, McLaren CE, Loreal O. Haemochromatosis. *Nat Rev Dis Primers* 2018;4:18016.
- 4) Wang CY, Babitt JL. Liver iron sensing and body iron homeostasis. *Blood* 2019;133:18-29.
- 5) Canali S, Zumbrennen-Bullough KB, Core AB, Wang CY, Nairz M, Bouley R, et al. Endothelial cells produce bone morphogenetic protein 6 required for iron homeostasis in mice. *Blood* 2017;129:405-414.
- 6) Canali S, Wang CY, Zumbrennen-Bullough KB, Bayer A, Babitt JL. Bone morphogenetic protein 2 controls iron homeostasis in mice independent of *Bmp6*. *Am J Hematol* 2017;92:1204-1213.
- 7) Koch PS, Olsavszky V, Ulbrich F, Sticht C, Demory A, Leibing T, et al. Angiocrine *Bmp2* signaling in murine liver controls normal iron homeostasis. *Blood* 2017;129:415-419.
- 8) Corradini E, Garuti C, Montosi G, Ventura P, Andriopoulos B Jr., Lin HY, et al. Bone morphogenetic protein signaling is impaired in an HFE knockout mouse model of hemochromatosis. *Gastroenterology* 2009;137:1489-1497.
- 9) Wallace DF, Summerville L, Crampton EM, Frazer DM, Anderson GJ, Subramaniam VN. Combined deletion of *Hfe* and transferrin receptor 2 in mice leads to marked dysregulation of hepcidin and iron overload. *HEPATOLOGY* 2009;50:1992-2000.
- 10) Ryan JD, Ryan E, Fabre A, Lawless MW, Crowe J. Defective bone morphogenetic protein signaling underlies hepcidin deficiency in HFE hereditary hemochromatosis. *HEPATOLOGY* 2010;52:1266-1273.
- 11) Corradini E, Rozier M, Meynard D, Odhiambo A, Lin HY, Feng Q, et al. Iron regulation of hepcidin despite attenuated *Smad 1,5,8* signaling in mice without transferrin receptor 2 or *Hfe*. *Gastroenterology* 2011;141:1907-1914.
- 12) Muckenthaler MU, Rivella S, Hentze MW, Galy B. A red carpet for iron metabolism. *Cell* 2017;168:344-361.
- 13) Hou Y, Zhang S, Wang L, Li J, Qu G, He J, et al. Estrogen regulates iron homeostasis through governing hepcidin expression via an estrogen response element. *Gene* 2012;511:398-403.
- 14) Yang Q, Jian J, Katz S, Abramson SB, Huang X. 17 β -Estradiol inhibits iron hormone hepcidin through an estrogen responsive element half-site. *Endocrinology* 2012;153:3170-3178.
- 15) Latour C, Kautz L, Besson-Fournier C, Island ML, Canonne-Hergaux F, Loreal O, et al. Testosterone perturbs systemic iron

- balance through activation of epidermal growth factor receptor signaling in the liver and repression of hepcidin. *HEPATOLOGY* 2014;59:683-694.
- 16) Guo W, Bachman E, Li M, Roy CN, Blusztajn J, Wong S, et al. Testosterone administration inhibits hepcidin transcription and is associated with increased iron incorporation into red blood cells. *Aging Cell* 2013;12:280-291.
 - 17) Goodnough JB, Ramos E, Nemeth E, Ganz T. Inhibition of hepcidin transcription by growth factors. *HEPATOLOGY* 2012;56:291-299.
 - 18) **Besson-Fournier C, Latour C, Kautz L, Bertrand J, Ganz T, Roth MP, et al.** Induction of activin B by inflammatory stimuli up-regulates expression of the iron-regulatory peptide hepcidin through Smad1/5/8 signaling. *Blood* 2012;120:431-439.
 - 19) Canali S, Core AB, Zumbrennen-Bullough KB, Merkulova M, Wang CY, Schneyer AL, et al. Activin B induces noncanonical SMAD1/5/8 signaling via BMP type I receptors in hepatocytes: evidence for a role in hepcidin induction by inflammation in male mice. *Endocrinology* 2016;157:1146-1162.
 - 20) **Wang RH, Li C, Xu X, Zheng Y, Xiao C, Zervas P, et al.** A role of SMAD4 in iron metabolism through the positive regulation of hepcidin expression. *Cell Metab* 2005;2:399-409.
 - 21) Theurl I, Schroll A, Sonnweber T, Nairz M, Theurl M, Willenbacher W, et al. Pharmacologic inhibition of hepcidin expression reverses anemia of chronic inflammation in rats. *Blood* 2011;118:4977-4984.
 - 22) **Steinbicker AU, Sachidanandan C, Vonner AJ, Yusuf RZ, Deng DY, Lai CS, et al.** Inhibition of bone morphogenetic protein signaling attenuates anemia associated with inflammation. *Blood* 2011;117:4915-4923.
 - 23) Mayeur C, Lohmeyer LK, Leyton P, Kao SM, Pappas AE, Kolodziej SA, et al. The type I BMP receptor Alk3 is required for the induction of hepatic hepcidin gene expression by interleukin-6. *Blood* 2014;123:2261-2268.
 - 24) **Besson-Fournier C, Gineste A, Latour C, Gourbeyre O, Meynard D, Martin P, et al.** Hepcidin upregulation by inflammation is independent of Smad1/5/8 signaling by activin B. *Blood* 2017;129:533-536.
 - 25) Verga Falzacappa MV, Casanovas G, Hentze MW, Muckenthaler MU. A bone morphogenetic protein (BMP)-responsive element in the hepcidin promoter controls HFE2-mediated hepatic hepcidin expression and its response to IL-6 in cultured cells. *J Mol Med (Berl)* 2008;86:531-540.
 - 26) Latour C, Besson-Fournier C, Gourbeyre O, Meynard D, Roth MP, Coppin H. Deletion of BMP6 worsens the phenotype of HJV-deficient mice and attenuates hepcidin levels reached after LPS challenge. *Blood* 2017;130:2339-2343.
 - 27) Wang CY, Core AB, Canali S, Zumbrennen-Bullough KB, Ozer S, Umans L, et al. Smad1/5 is required for erythropoietin-mediated suppression of hepcidin in mice. *Blood* 2017;130:73-83.
 - 28) Tsukamoto S, Mizuta T, Fujimoto M, Ohte S, Osawa K, Miyamoto A, et al. Smad9 is a new type of transcriptional regulator in bone morphogenetic protein signaling. *Sci Rep* 2014;4:7596.
 - 29) Arnold SJ, Maretto S, Islam A, Bikoff EK, Robertson EJ. Dose-dependent Smad1, Smad5 and Smad8 signaling in the early mouse embryo. *Dev Biol* 2006;296:104-118.
 - 30) **Kautz L, Meynard D, Monnier A, Darnaud V, Bouvet R, Wang RH, et al.** Iron regulates phosphorylation of Smad1/5/8 and gene expression of Bmp6, Smad 7, Id1, and Atoh8 in the mouse liver. *Blood* 2008;112:1503-1509.
 - 31) Lebeau A, Frank J, Biesalski HK, Weiss G, Srai SK, Simpson RJ, et al. Long-term sequelae of HFE deletion in C57BL/6 × 129/O1a mice, an animal model for hereditary haemochromatosis. *Eur J Clin Invest* 2002;32:603-612.
 - 32) Lunova M, Goehring C, Kucuoglu D, Mueller K, Chen Y, Walthers P, et al. Hepcidin knockout mice fed with iron-rich diet develop chronic liver injury and liver fibrosis due to lysosomal iron overload. *J Hepatol* 2014;61:633-641.
 - 33) Delima RD, Chua AC, Tirnitz-Parker JE, Gan EK, Croft KD, Graham RM, et al. Disruption of hemochromatosis protein and transferrin receptor 2 causes iron-induced liver injury in mice. *HEPATOLOGY* 2012;56:585-593.
 - 34) Padda RS, Gkouvatso K, Guido M, Mui J, Vali H, Pantopoulos K. A high-fat diet modulates iron metabolism but does not promote liver fibrosis in hemochromatotic HJV^{-/-} mice. *Am J Physiol Gastrointest Liver Physiol* 2015;308:G251-G261.
 - 35) Fleming RE, Holden CC, Tomatsu S, Waheed A, Brunt EM, Britton RS, et al. Mouse strain differences determine severity of iron accumulation in Hfe knockout model of hereditary hemochromatosis. *Proc Natl Acad Sci USA* 2001;98:2707-2711.
 - 36) Babitt JL, Huang FW, Wrighting DM, Xia Y, Sidis Y, Samad TA, et al. Bone morphogenetic protein signaling by hemojuvelin regulates hepcidin expression. *Nat Genet* 2006;38:531-539.
 - 37) **Meynard D, Kautz L, Darnaud V, Canonne-Hergaux F, Coppin H, Roth MP.** Lack of the bone morphogenetic protein BMP6 induces massive iron overload. *Nat Genet* 2009;41:478-481.
 - 38) Niederkofler V, Salie R, Arber S. Hemojuvelin is essential for dietary iron sensing, and its mutation leads to severe iron overload. *J Clin Invest* 2005;115:2180-2186.
 - 39) Miyazono K, Kamiya Y, Morikawa M. Bone morphogenetic protein receptors and signal transduction. *J Biochem* 2010;147:35-51.
 - 40) Fargion S, Valenti L, Fracanzani AL. Beyond hereditary hemochromatosis: new insights into the relationship between iron overload and chronic liver diseases. *Dig Liver Dis* 2011;43:89-95.
- Author names in bold designate shared co-first authorship.

Supporting Information

Additional Supporting Information may be found at onlinelibrary.wiley.com/doi/10.1002/hep.30780/supinfo.